Supplementary Material (ESI) for CrystEngComm

A Case Study of the Zn^{II}-BDC/bpt Mixed-Ligand System: Positional Isomeric Effect, Structural Diversification and Luminescent Properties

Fu-Ping Huang, Jin-Lei Tian, Gong-Jun Chen, Dong-Dong Li, Wen Gu, Xin Liu, Shi-Ping Yan, Dai-Zheng Liao, Peng Cheng

Department of Chemistry,
Nankai University, Tianjin 300071,
P R China. E-mail: yansp@nankai.edu.cn

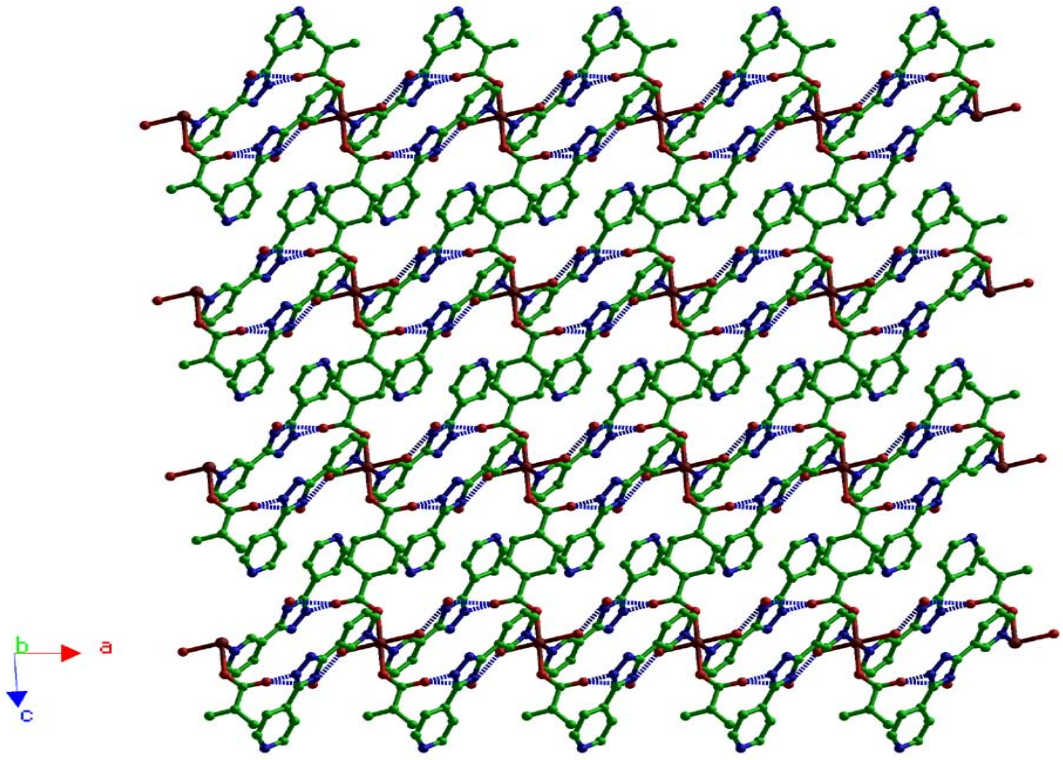

Figure S1. The 3-D network structure of complex **2**

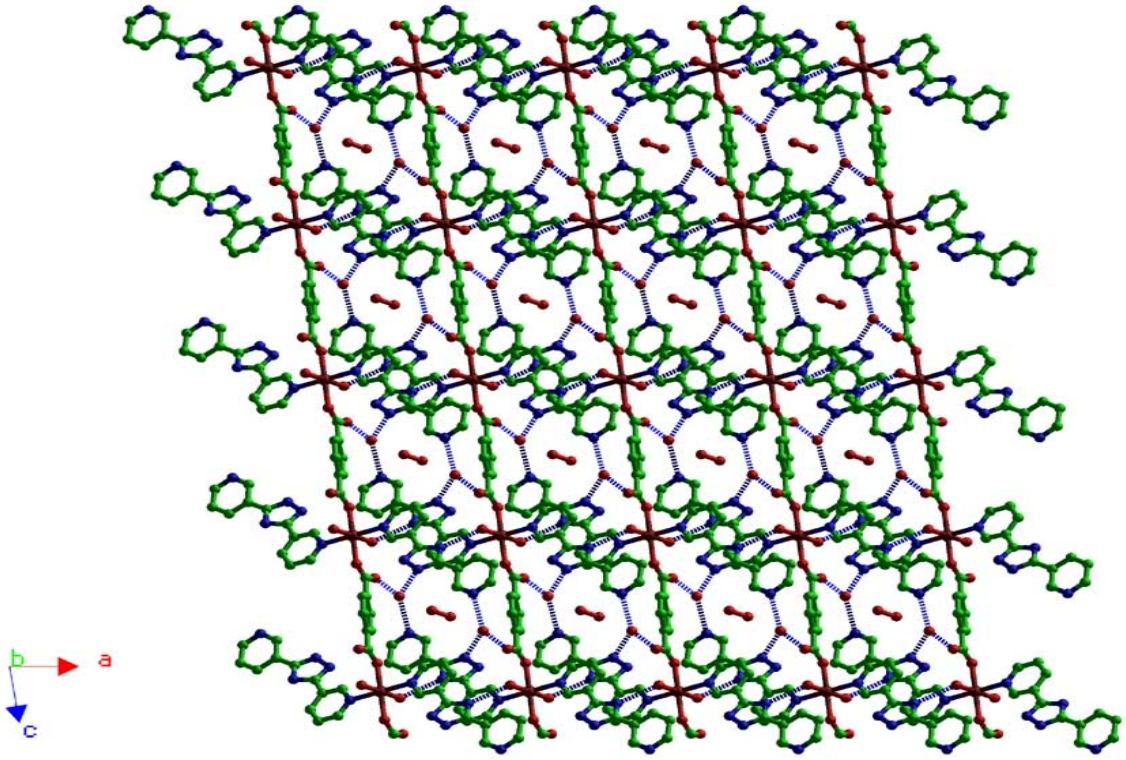

Figure S2. The 3-D network structure of complex **3**

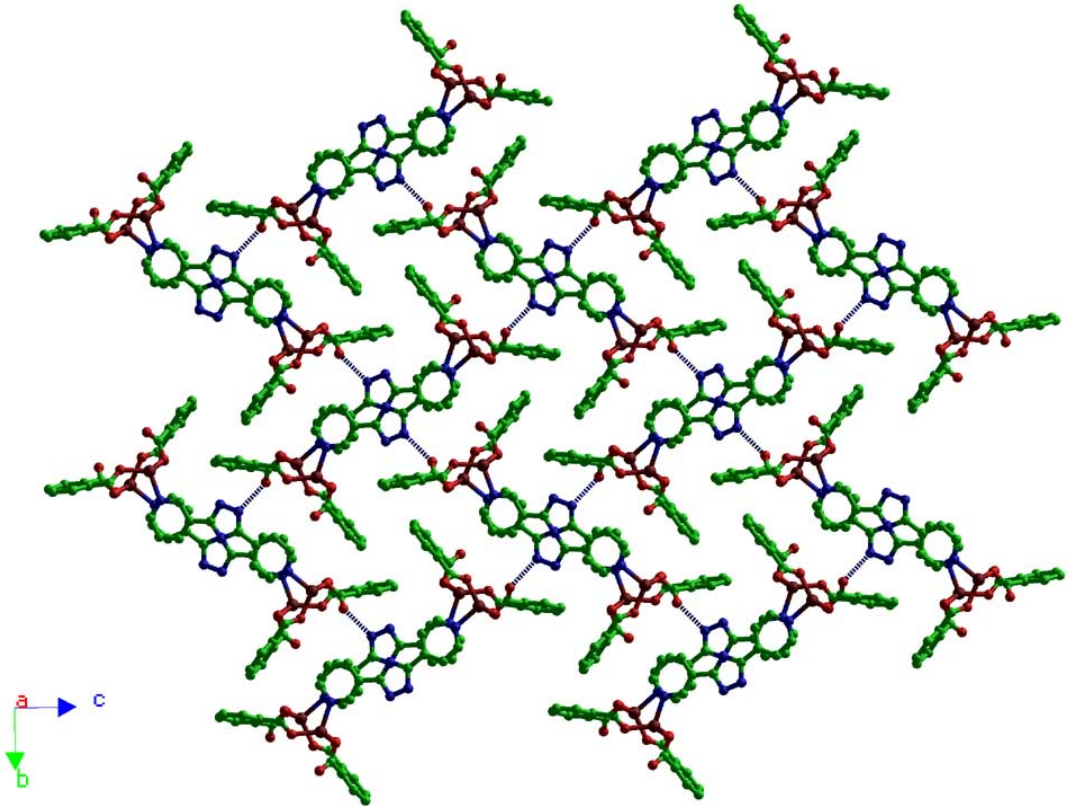

Figure S3. The 3-D network structure of complex **8**

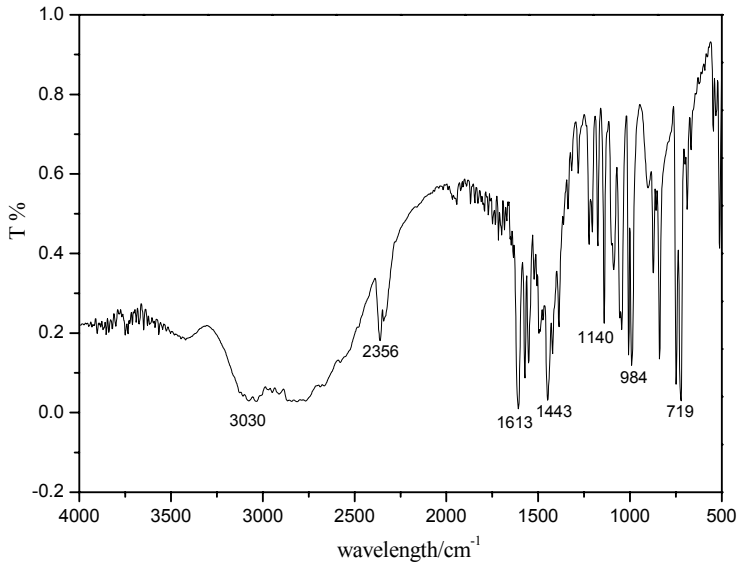

Figure S4. The IR spectra for the free ligand (4,4′-bpt)

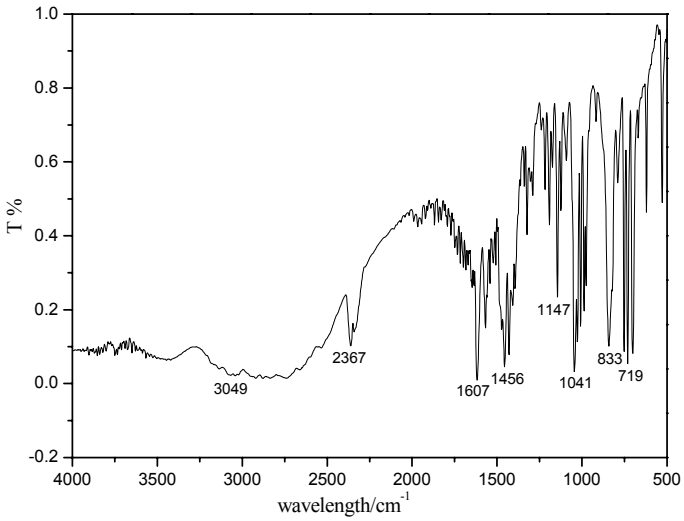

Figure S5. The IR spectra for the free ligand (3,4′-bpt)

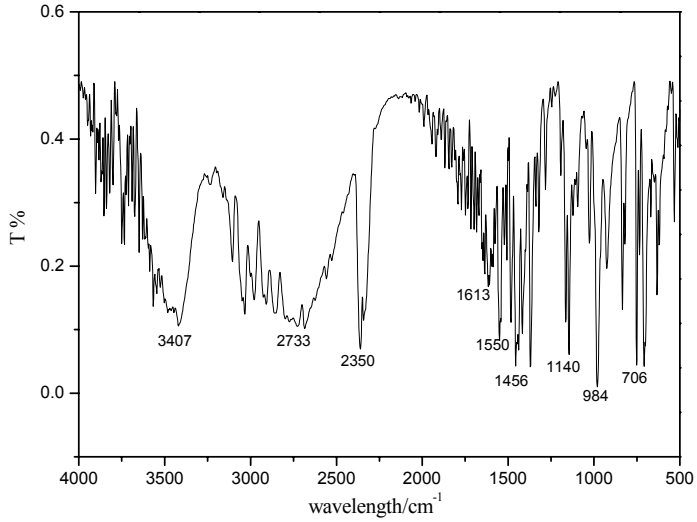

Figure S6. The IR spectra for the free ligand (3,3′-bpt)

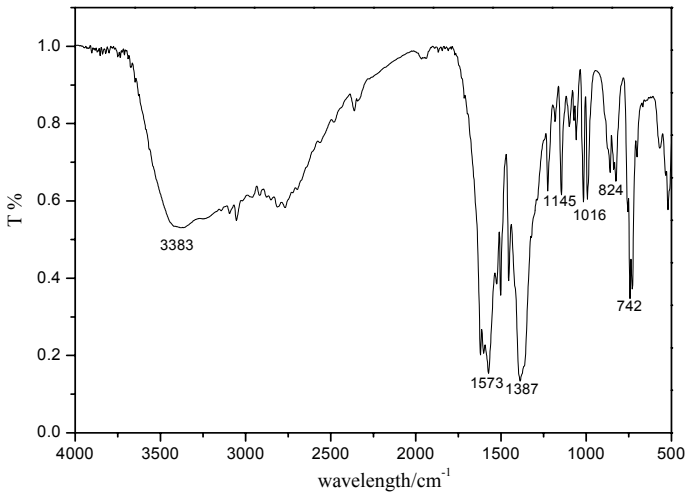

Figure S7. The IR spectra of complex **1**

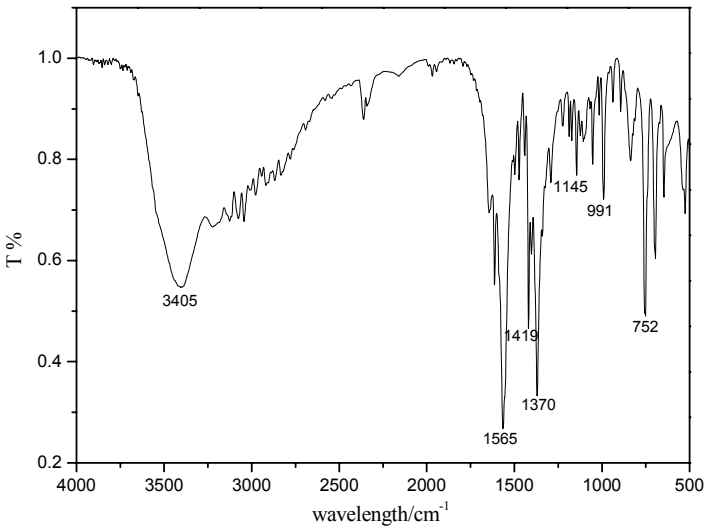

Figure S8. The IR spectra of complex **2**

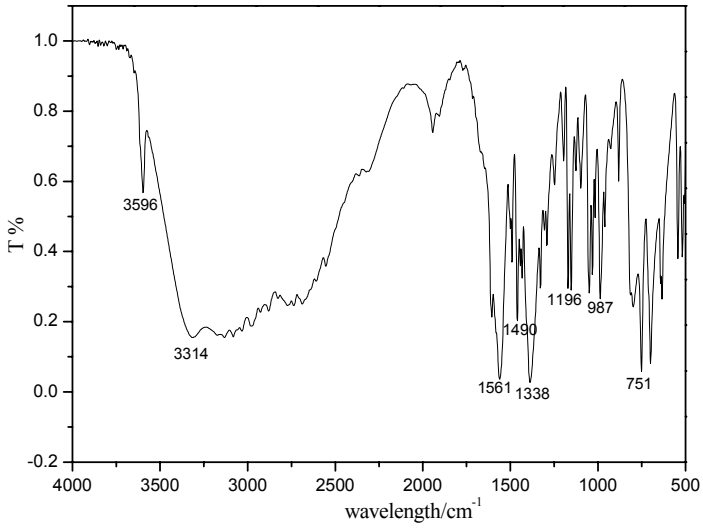

Figure S9. The IR spectra of complex **3**

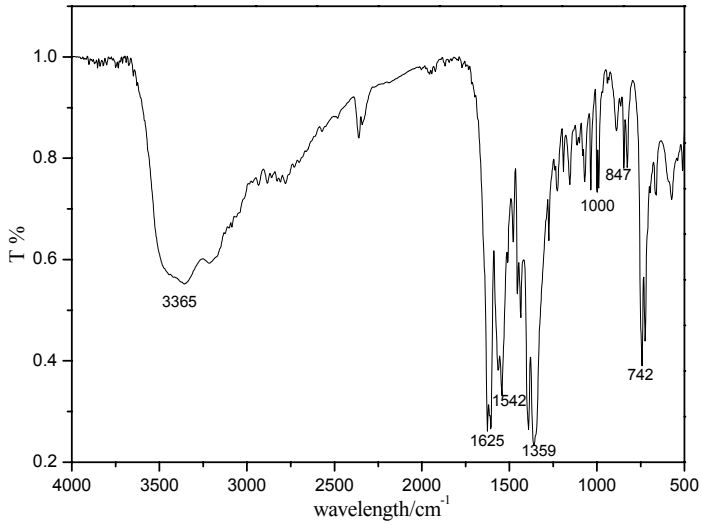

Figure S10. The IR spectra of complex **4**

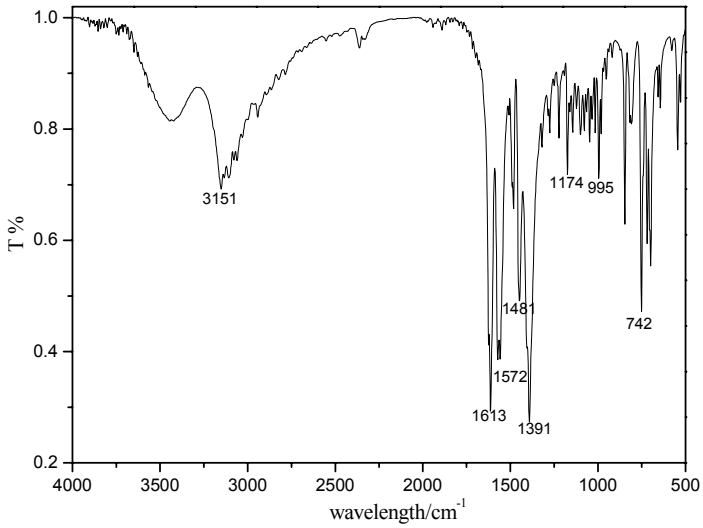

Figure S11. The IR spectra of complex **5**

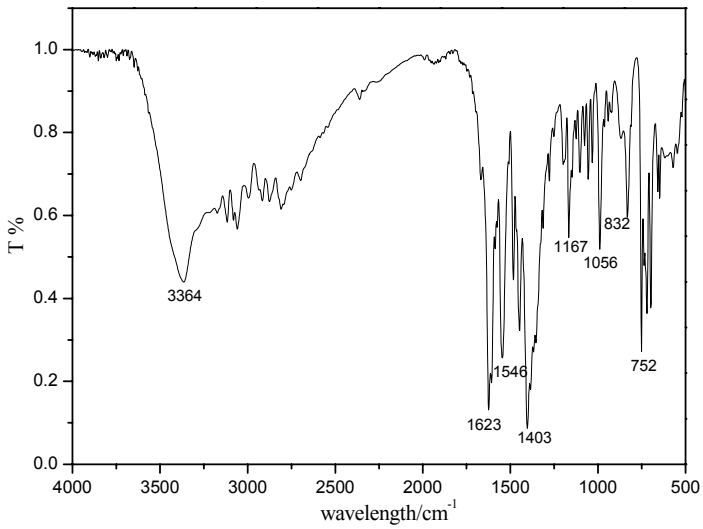

Figure S12. The IR spectra of complex **6**

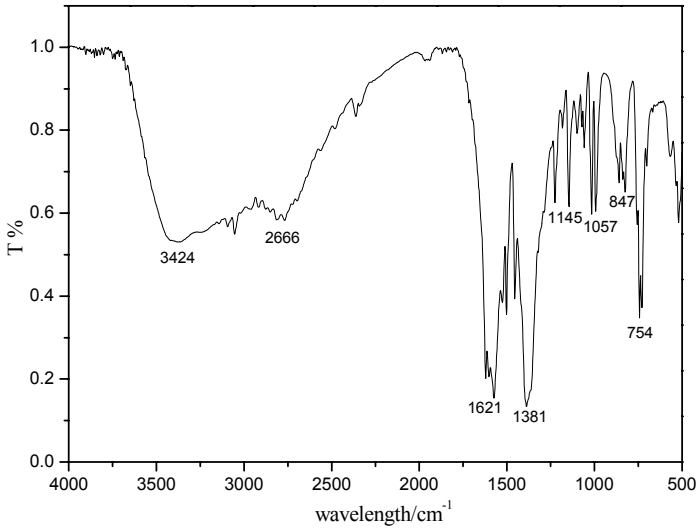

Figure S13. The IR spectra of complex **7**

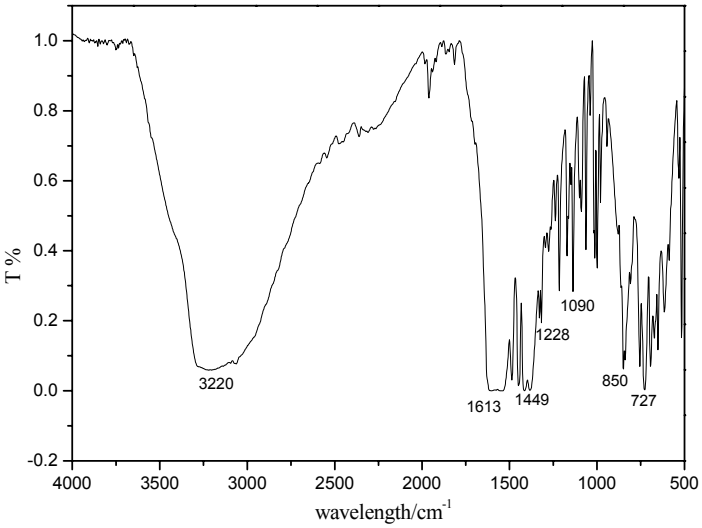

Figure S14. The IR spectra of complex **8**

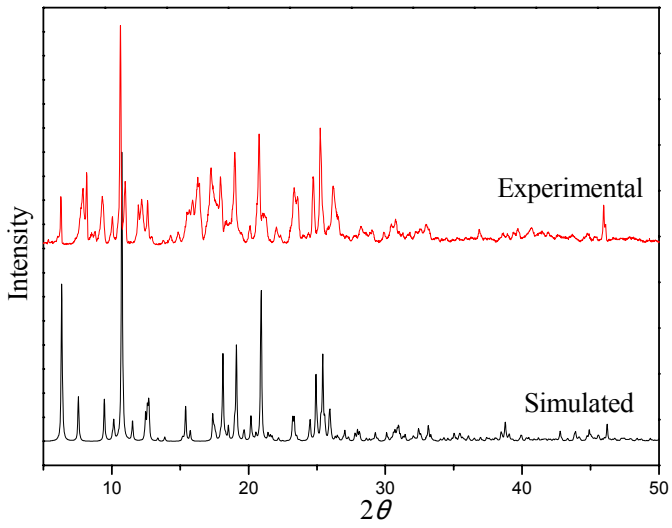

Figure S15. Measured and calculated X-ray powder diffraction (XRD) pattern of **1**

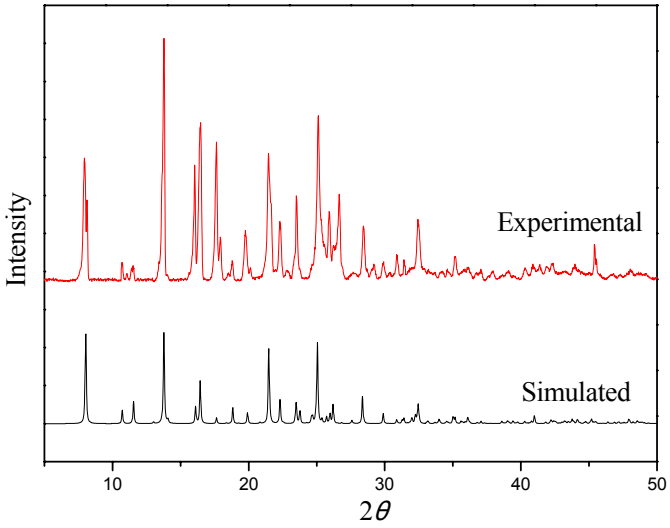

Figure S16. Measured and calculated X-ray powder diffraction (XRD) pattern of **2**

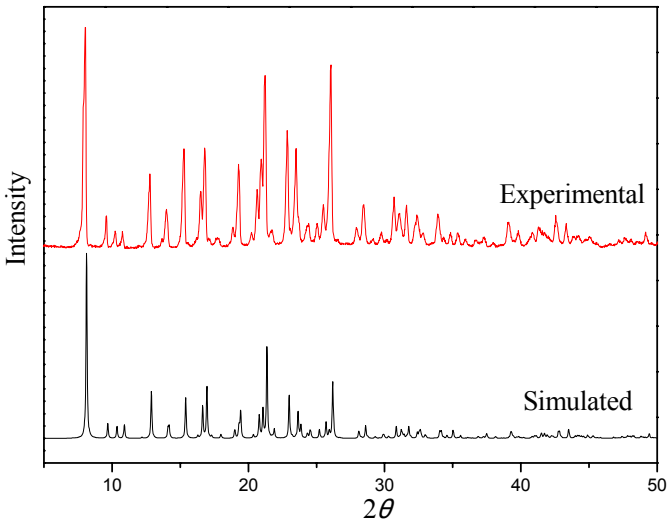

Figure S17. Measured and calculated X-ray powder diffraction (XRD) pattern of **3**

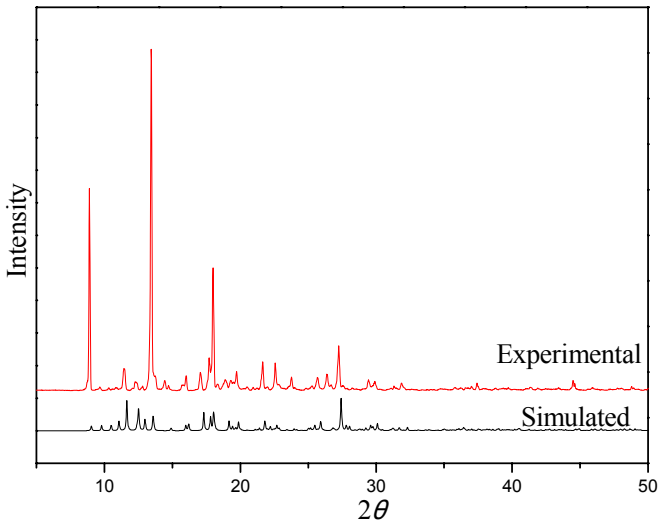

Figure S18. Measured and calculated X-ray powder diffraction (XRD) pattern of **4**

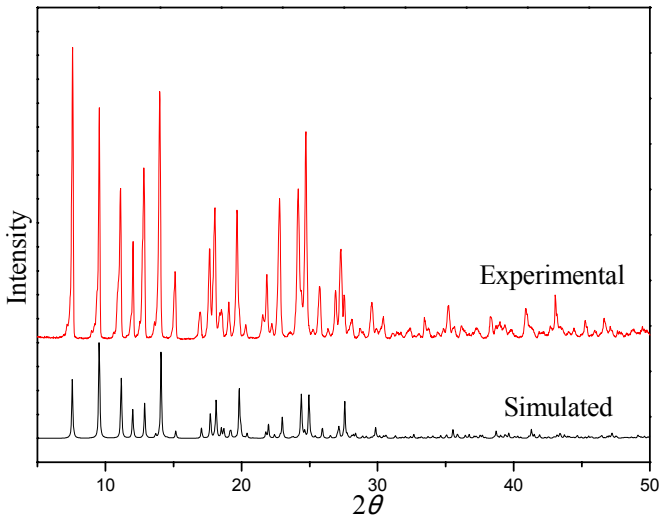

Figure S19. Measured and calculated X-ray powder diffraction (XRD) pattern of **5**

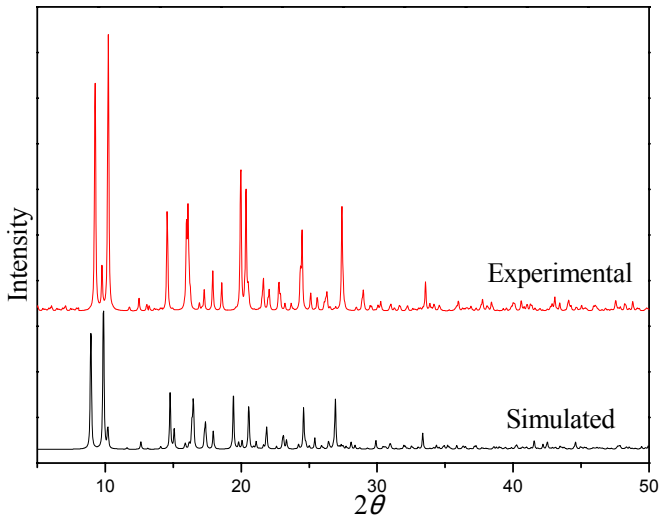

Figure S20. Measured and calculated X-ray powder diffraction (XRD) pattern of **6**

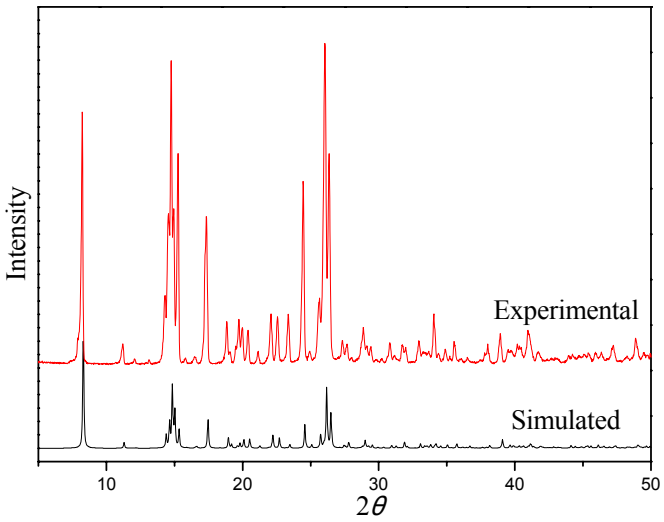

Figure S21. Measured and calculated X-ray powder diffraction (XRD) pattern of **7**

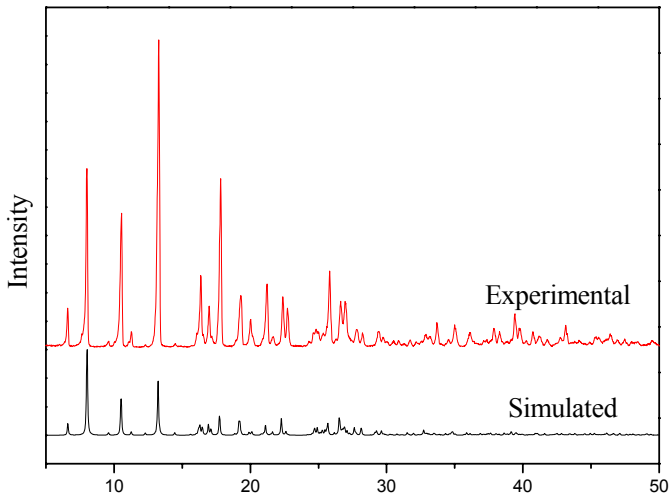

Figure S22. Measured and calculated X-ray powder diffraction (XRD) pattern of **8**

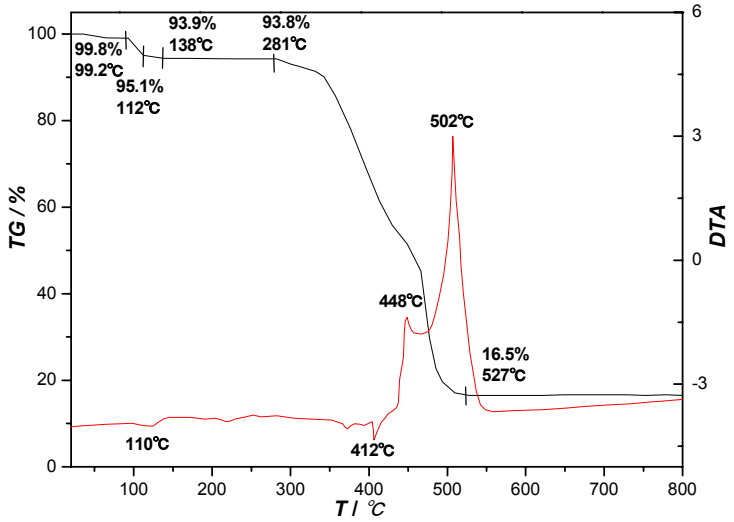

Figure S23. The TG (black)-DTA (red) curve of complex **1**

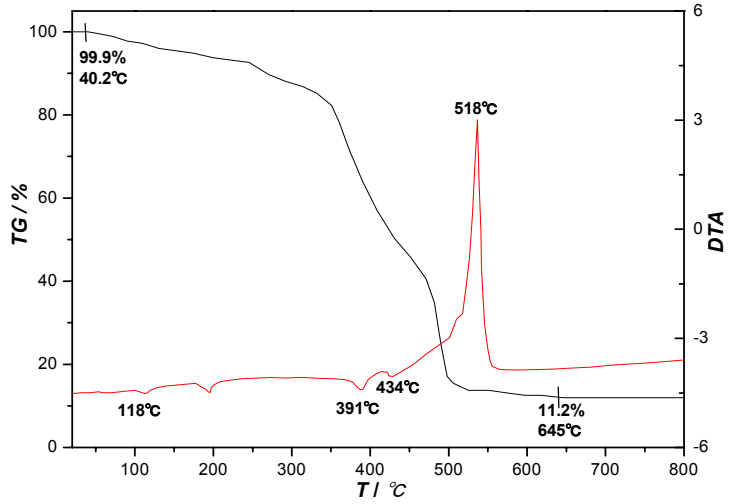

Figure S24. The TG (black)-DTA (red) curve of complex **2**

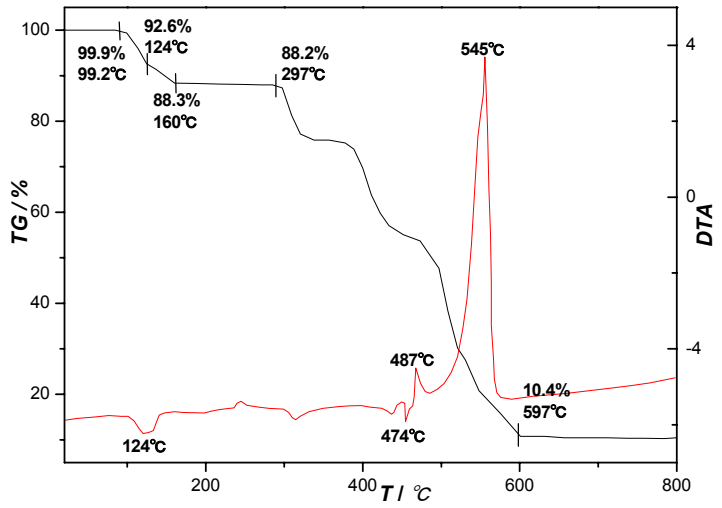

Figure S25. The TG (black)-DTA (red) curve of complex **3**

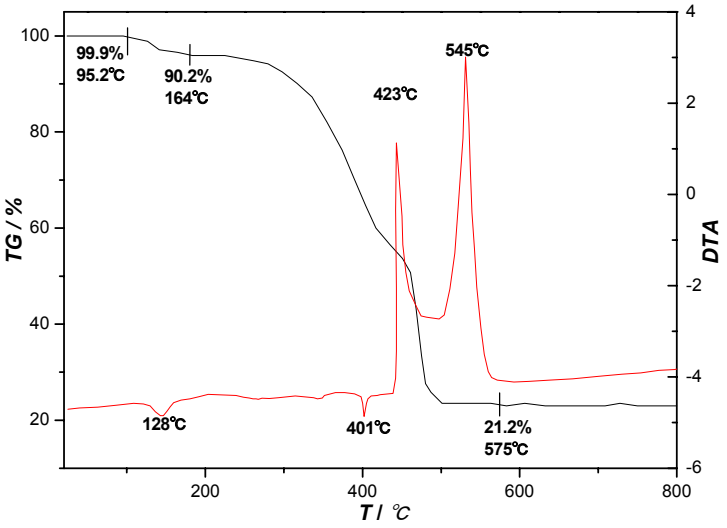

Figure S26. The TG (black)-DTA (red) curve of complex **4**

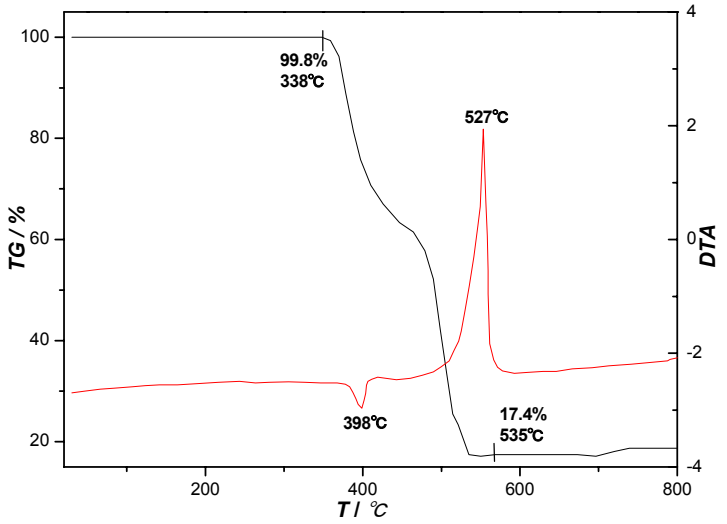

Figure S27. The TG (black)-DTA (red) curve of complex **5**

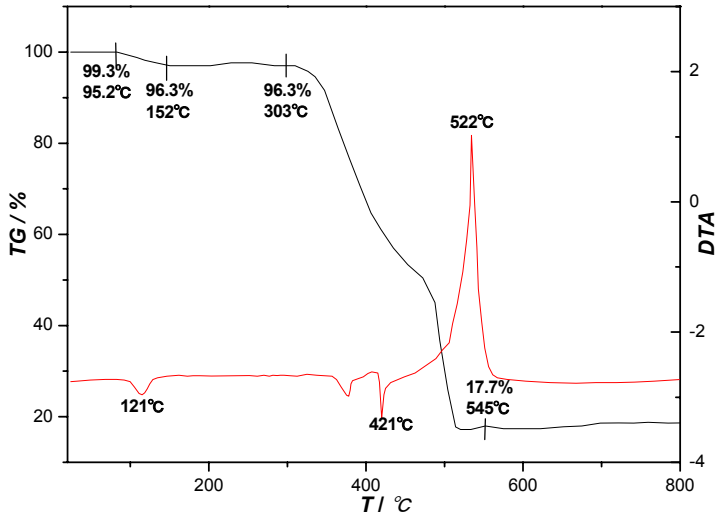

Figure S28. The TG (black)-DTA (red) curve of complex **6**

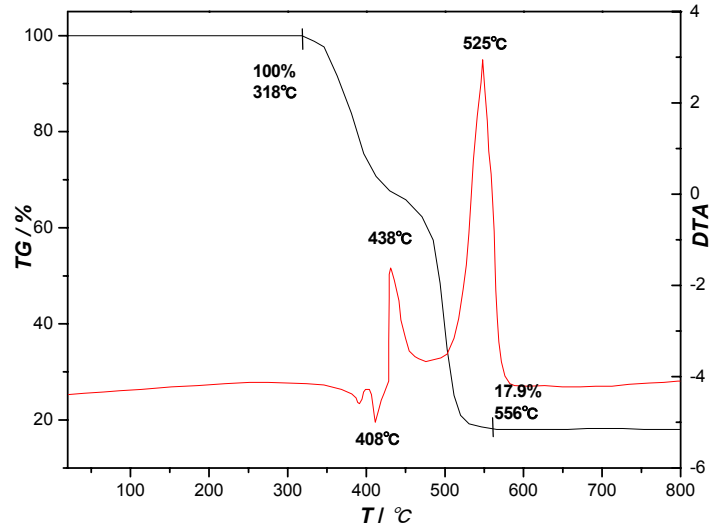

Figure S29. The TG (black)-DTA (red) curve of complex **7**

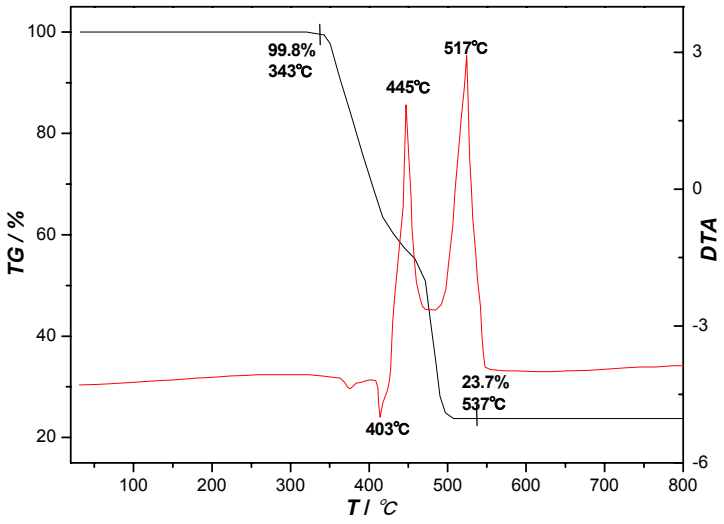

Figure S30. The TG (black)-DTA (red) curve of complex **8**

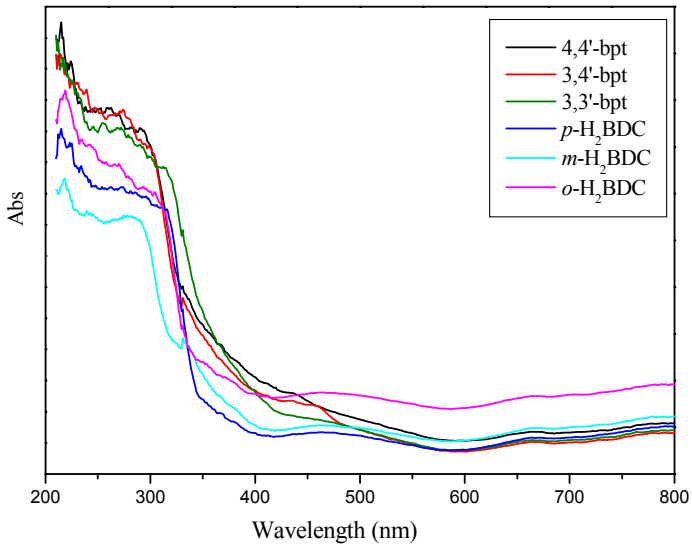

Figure S31. Solid state UV-vis spectra for free ligands (*p*-H_2BDC, *m*-H_2BDC, *o*-H_2BDC, 4,4′-bpt, 3,4′-bpt and 3,3′-bpt) at room temperature

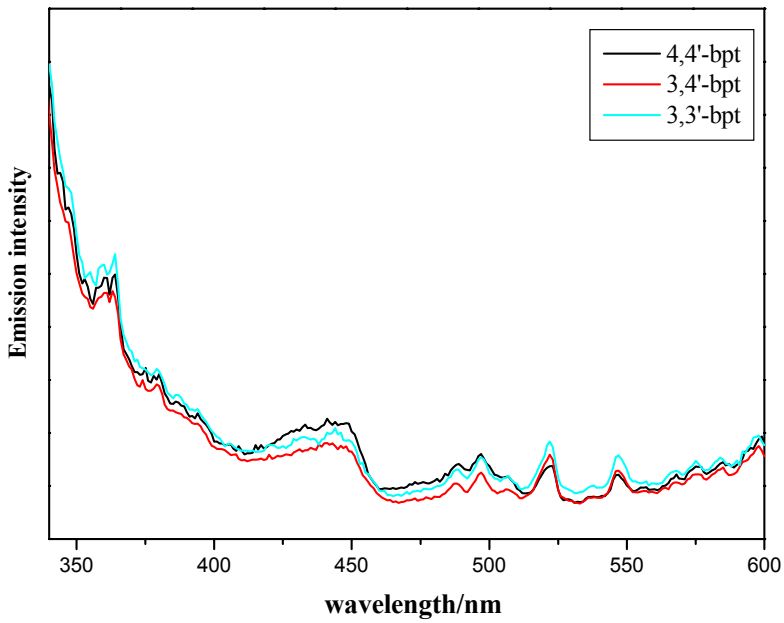

Figure S32. Solid-state fluorescence emissions recorded for free ligands (4,4′-bpt, 3,4′-bpt and 3,3′-bpt) at room temperature

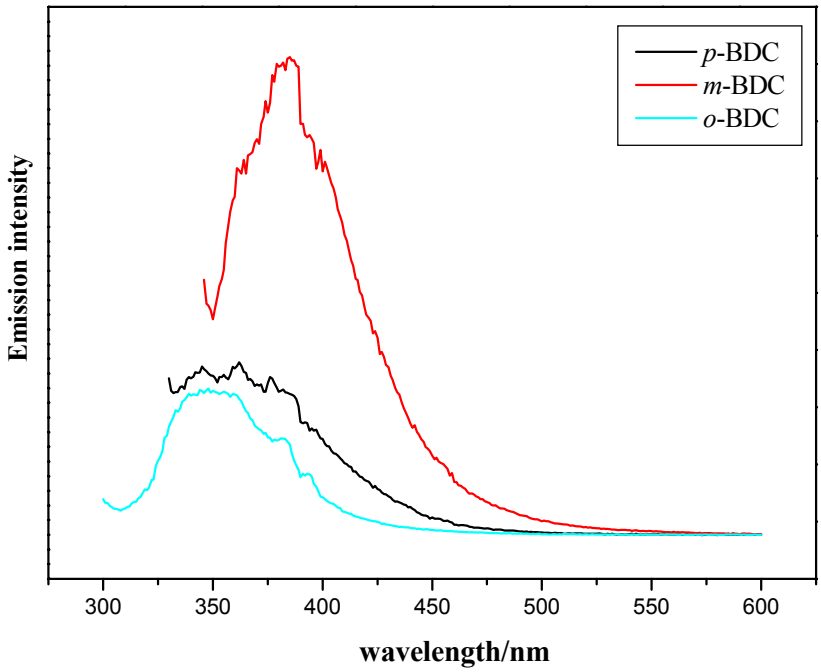

Figure S33. Solid-state fluorescence emissions recorded for free ligands (*p*-H_2BDC, *m*-H_2BDC and *o*-H_2BDC,) at room temperature